EBioMedicine 4 (2016) 50–61

Contents lists available at ScienceDirect

EBioMedicine

journal homepage: www.ebiomedicine.com

Research Paper

Modulation of mTOR Signalling Triggers the Formation of Stem Cell-like Memory T Cells

Godehard Scholz [a], Camilla Jandus [a], Lianjun Zhang [a], Camille Grandclément [b], Isabel C. Lopez-Mejia [c], Charlotte Soneson [d], Mauro Delorenzi [d,e,f], Lluis Fajas [c], Werner Held [b], Olivier Dormond [g], Pedro Romero [a,f,*]

[a] Translational Tumor Immunology Group, Ludwig Cancer Research (LICR), University of Lausanne (UNIL), 1066 Epalinges, Vaud, Switzerland
[b] Lymphocyte Function Group, LICR, UNIL, Switzerland
[c] Department of Physiology, UNIL, 1015 Lausanne, Vaud, Switzerland
[d] Bioinformatics Core Facility, Swiss Institute of Bioinformatics, UNIL, Switzerland
[e] LICR, UNIL, Switzerland
[f] Department of Oncology, Lausanne University Hospital (CHUV), 1011 Lausanne, Vaud, Switzerland
[g] Department of Visceral Surgery, CHUV, Switzerland

ARTICLE INFO

Article history:
Received 26 June 2015
Received in revised form 23 December 2015
Accepted 14 January 2016
Available online 16 January 2016

Keywords:
Human T cells
T cell differentiation
Adoptive cell transfer therapy
Rapamycin

ABSTRACT

Robust, long-lasting immune responses are elicited by memory T cells that possess properties of stem cells, enabling them to persist long-term and to permanently replenish the effector pools. Thus, stem cell-like memory T (T_{SCM}) cells are of key therapeutic value and efforts are underway to characterize T_{SCM} cells and to identify means for their targeted induction.

Here, we show that inhibition of mechanistic/mammalian Target of Rapamycin (mTOR) complex 1 (mTORC1) by rapamycin or the Wnt-β-catenin signalling activator TWS119 in activated human naive T cells leads to the induction of T_{SCM} cells. We show that these compounds switch T cell metabolism to fatty acid oxidation as favoured metabolic programme for T_{SCM} cell generation. Of note, pharmacologically induced T_{SCM} cells possess superior functional features as a long-term repopulation capacity after adoptive transfer. Furthermore, we provide insights into the transcriptome of T_{SCM} cells.

Our data identify a mechanism of pharmacological mTORC1 inhibitors, allowing us to confer stemness to human naive T cells which may be significantly relevant for the design of innovative T cell-based cancer immunotherapies.

1. Introduction

Similar to solid organs, T cells have been suggested to harbour a self-renewing stem cell-like population which permanently replenishes the pools of further differentiated effectors. Since central memory T (T_{CM}) cells have been shown to repopulate the effector memory T (T_{EM}) cell and effector T (T_{EFF}) cell pools in response to antigen stimulus (Graef et al., 2014; Wherry et al., 2003), they were thus far regarded as "memory stem cells". However, further complexity was brought to this view by the recent discovery of an additional memory T cell subset, which was able to mediate a prolonged immune response in a mouse model of graft-*versus*-host disease (GVHD) (Zhang et al., 2005). This memory T cell subset, termed stem cell-like memory T (T_{SCM}) cells, has been recently described in mice, non-human primates and in humans (Gattinoni et al., 2009, 2011; Lugli et al., 2013). As least differentiated distinct memory T cell subset, T_{SCM} cells have been put at the top of the hierarchy of all memory T cell subsets in a model of progressive T cell differentiation, leading from naive T (T_N) cells over T_{SCM} cells and T_{CM} cells to T_{EM} cells and T_{EFF} cells. This position of T_{SCM} cells between T_N cells and memory T cells is phenotypically reflected by the expression of activation markers as the death receptor CD95, the β-chain of the IL-2 receptor (CD122) or the adhesion molecule CD58 on naive-appearing CCR7+, CD45RA+, CD45RO− T cells (Gattinoni et al., 2011). After genetic modification into mesothelioma-specific CAR T cells, adoptively transferred T_{SCM} cells were shown to mediate an improved anti-tumour immune response compared to T_N cells, T_{CM} cells and T_{EM} cells in a humanized mouse model (Gattinoni et al., 2011), which seems to depend on a more efficient T_{SCM} cell engraftment and long-term persistence in the host which enables them, while self-renewing, to constantly differentiate into T_{EFF} cells and, thereby, to completely eradicate the tumour.

Because of these ideal characteristics there is a quest for the signalling pathways which mediate T_{SCM} cell induction. Once identified, pharmacological interference with these signalling pathways could be used for their targeted induction in anti-tumour immunotherapy. In this regard, the *in vitro* activation of CD8+ T_N cells in the presence of the

* Corresponding author at: Translational Tumor Immunology Group, Ludwig Cancer Research (LICR), University of Lausanne (UNIL), 1066 Epalinges, Vaud, Switzerland.
E-mail address: Pedro.Romero@unil.ch (P. Romero).

http://dx.doi.org/10.1016/j.ebiom.2016.01.019

Wnt-β-catenin (short: Wnt) signalling pathway activator TWS119, which inhibits glycogen synthase kinase-3β (GSK-3β) by phosphorylation, has been suggested to arrest T_N cell differentiation and to generate T_{SCM} cells (Gattinoni et al., 2011). However, the interpretability of these data remains inconclusive, since the starting pool of T_N cells also contained T_{SCM} cells so that an expansion effect of TWS119 on pre-existing T_{SCM} cells or T_{SCM} cell self-maintaining factors cannot be excluded. Moreover, increasing evidence suggests that T cell metabolism is an important determinant of T cell differentiation (Pearce et al., 2009), which raises the possibility that metabolic integrators like mechanistic/mammalian Target Of Rapamycin (mTOR) kinase might represent pharmacological targets for the enrichment of a desired differentiation-defined T cell population (Araki et al., 2009; Diken et al., 2013; Rao et al., 2010; Turner et al., 2011), thereby potentially favouring the induction of qualitatively improved memory T cells.

We, therefore, set out to investigate whether mTORC1 inhibitors like rapamycin would be relevant for the generation of human T_{SCM} cells and whether a cross-talk between mTOR and Wnt signalling would exist. Moreover, since current knowledge on the generation and characterization of T_{SCM} cells remains limited to CD8 + T_{SCM} cells, apart from their phenotypic definition, CD4 + T_{SCM} cells remain uninvestigated. The characterization of CD4 + T_{SCM} cells seems to be of great importance all the more, as the role of CD4 + T cells as broad orchestrators of the immune response receives growing attention in anti-tumour immunotherapy (Kamphorst and Ahmed, 2013; Muranski and Restifo, 2009). In the present study, therefore, focus was put on the induction and characterization of CD4 + T_{SCM} cells, nevertheless testing the relevance of our findings on T_{SCM} cell induction also for CD8 + T_{SCM} cells.

Here, we revealed the inhibition of mTORC1 with simultaneously active mTORC2 signalling as the molecular mechanism inducing T_{SCM} cells and that T_{SCM} cell induction takes place in complete independence from Wnt signalling. We furthermore present insights into the transcriptomes of naturally occurring and pharmacologically induced CD4 + T_{SCM} cells, the *in vivo* survival and repopulation capacity of pharmacologically induced CD4 + T_{SCM} cells and the metabolic regulation of CD4 + T_{SCM} cell generation. Taken together, our findings are of direct relevance for the design of improved anti-tumour immunotherapies.

2. Materials & Methods

2.1. Human T Lymphocytes

Peripheral blood mononuclear cells (PBMCs) were isolated by density centrifugation over a Ficoll-Paque gradient (Lymphoprep™) from buffy coats of healthy human female and male blood donors, obtained from the Vaud blood transfusion service. Experiments were performed in accordance to the guidelines of the Ethics Commission of the UNIL. Prior to sorting, PBMCs were purified with CD3, CD4 or CD8 Dynabeads® (Invitrogen™).

2.2. Animal Experiments

Animal experiments were performed in accordance to the guidelines of the Ethics Commission of the UNIL. *In vitro* experiments and assessment of T_{SCM} cell frequencies were performed with female Raptor (CD4-Cre), β-/γ-catenin (Vav-Cre) KO mice and their corresponding WT forms. Adoptive T cell transfer was conducted with female NOD.Cg-Prkdc^{scid}Il2rg^{tm1Wjl}/SzJ mice (NSG).

2.3. Cell Culture

T cells were cultured in RPMI-1640 supplemented with 8% heat inactivated, pooled human serum or 10% foetal calf serum, 50 IU/ml penicillin, 50 μg/ml streptomycin, 4 mM L-glutamine, 1% (v/v) non-essential amino acids and 50 μM 2-mercaptoethanol. Sorted T_N cells were primed with anti-CD3/CD28 beads (Invitrogen) or OKT3/anti-CD28 antibody (in house, derived from hybridoma cells) and IL-2 (Proleukin®, Roche Pharma AG). Pathway interfering drugs were TWS119 (Cayman Chemical), rapamycin (LC Laboratories), PP242 (Chemdea), KU-0063794 (Chemdea), Indirubin-3-monoxime (Sigma-Aldrich), SB216763 (Sigma-Aldrich) and recombinant human Wnt3A (R&D Systems).

2.4. Flow Cytometry

Flow cytometry acquisition was performed with a Gallios™ (Beckman Coulter) or a LSR II flow cytometer (BD Biosciences). Cell sorting was conducted with a FACS Aria (BD Biosciences) or a MoFlo® Astrios™ cell sorting instrument (Beckman Coulter). Flow cytometry analysis was performed with FlowJo software (Version 7.6.5, Treestar).

Antibodies and staining panels are listed in the *Supplemental Experimental Procedures*.

2.5. Phospho-specific Flow Cytometry

1,000,000 T_N cells were sorted per condition. After activation with anti-CD3/CD28 beads (1:1 bead/cell ratio) in the presence of TWS119 (5 μM) or rapamycin (100 nM) for 4 h, T_N cells were harvested, fixed and incubated with ice-cold 50% methanol for membrane permeabilization. Primary antibodies were pS6 ribosomal protein (Ser235/236), pGSK-3β (Ser9), pAKT (Ser473), p4EBP1 (Ser65), p4EBP1 (Thr37/46) (all from Cell Signaling). The secondary antibody was Alexa Fluor 647 goat anti rabbit IgG (Life Technologies).

2.6. Western Blot Analysis

For Western blot analysis activated (4 h in presence of indicated drugs) natural (n) CD4 + T_N cells were washed in ice-cold PBS and lysed in RIPA buffer containing protease inhibitor and sodium orthovanadate (Santa Cruz Biotechnologies). Proteins were separated by 4% to 12% polyacrylamide gel and transferred to a polyvinylidene difluoride membrane (Millipore). Membranes were blocked with Odyssey® blocking buffer (LI-COR Biosciences) and immunoblotted with the primary antibodies pS6 ribosomal protein (Ser235/236), pAKT (Ser473), β-actin (all from Cell Signaling) followed by infrared secondary antibodies. Bands from immunoreactive proteins were visualized by an Odyssey® infrared imaging system (LI-COR Biosciences).

2.7. RNA Sequencing

RNA sequencing was conducted with nCD4 + T_N, T_{SCM} and T_{CM} cells from 4 healthy human donors. Additionally, TWS119- and rapamycin-induced T_{SCM} cells were resorted after 14 days of nCD4 + T_N cell priming from the same donors. RNA was purified with Arcturus PicoPure RNA Isolation kit (Biosystems/Applied Life Technologies). An amount of 10 ng total RNA was amplified with the SMARTer Ultra Low RNA Kit for Illumina Sequencing (Clontech Laboratories, Inc.) and the Advantage 2 PCR Kit (Clontech Laboratories, Inc.). The cDNA from the amplification reactions was sheared with a Covaris ultrasonicator (Covaris, Inc.) and sequencing libraries were generated with a Truseq DNA kit (Illumina, Inc.). Libraries were sequenced at 100 nucleotides single read mode on an Illumina HiSeq 2000 instrument.

2.8. Adoptive T Cell Transfer

Adoptive T cell transfer was conducted by tail vein injection of 200,000 rapamycin-induced CD4 + T_{SCM} cells and equal numbers of CD4 + T_N-like and T_{CM}-like cells. Control mice received an equal volume of culture medium. Lymphocytes from lung and liver were isolated by Percoll™ technique.

2.9. Cell Proliferation Assay

30,000 rapamycin-induced CD4 + T_{SCM} cells and equal numbers of T_N- and T_{CM}-like cells were labelled for 6 days with carboxyfluorescein succinimidyl ester (CFSE, Life Technologies) (final concentration: 0.25 μM) and expanded in presence of IL-2 (50 IU/ml). Dilution of CFSE (488 nm) was assessed by flow cytometry. The proliferation index was calculated with ModFit LT software (Version 3.3.11, Verity Software House, Inc.).

2.10. MMP

Assessment of MMP was performed with TMRE — Mitochondrial Membrane Potential Assay Kit (Abcam®). 5,000,000 nCD4 + T cells and equal numbers of T cells derived from nCD4 + T_N cells, which have been activated for 14 days in presence of rapamycin (100 nM), were used. T cells were incubated with 100 nM tetramethylrhodamine, ethyl ester (TMRE) for 30 min at 37 °C in the water bath. Carbonyl cyanide-4-(trifluoromethoxy)phenylhydrazone (FCCP, 100 μM) was added during acquisition.

2.11. 2-NBDG Uptake

2-[N-(7-Nitrobenz-2-oxa-1,3-diazol-4-yl)amino]-2-deoxy-D-glucose (2-NBDG, Invitrogen) uptake was carried out with 5,000,000 nCD4 + T cells and equal numbers of T cells, derived from nCD4 + T_N cells, which have been activated for 14 days in presence of rapamycin (100 nM). T cells were incubated for 15 min at 37 °C in glucose-free Krebs-Ringer Hepes buffer (Hepes 50 mM, NaCl 137 mM, KCl 4.7 mM, $CaCl_2$ 1.85 mM, $MgSO_4$ 1.3 mM, BSA 0.1% w/v, pH 7.4). T cells were pelleted, washed and incubated with 100 μM 2-NBDG at 37 °C in the water bath prior to measuring fluorescence by flow cytometry.

2.12. Assessment of ECAR and OCR

For extracellular acidification rate (ECAR) and oxygen consumption rate (OCR) measurements we used an XF24 extracellular analyser (Seahorse™ Bioscience). T_N (750,000 per well) and T_{SCM} cells (200,000 per well) have been immobilized using CellTak™ agent (BD Biosciences). T cells were kept in non-buffered assay medium (KHB with 25 mM glucose, 1 mM sodium pyruvate, 2 mM glutamine for ECAR assessment or 2.5 mM glucose and 1.5 mM carnitine for OCR measurement) and incubated in a non-CO_2 incubator for 60 min at 37 °C prior to analysis. Anti-CD3/CD28 beads, TWS119, rapamycin, oligomycin and palmitate were added prior to or during the analysis at the indicated time points and concentrations. ECAR and OCR were calculated using Seahorse™ Bioscience proprietary software.

2.13. Statistical Analysis

2.13.1. Flow Cytometry

Statistical analysis was performed with Prism software (Version 6, GraphPad), using a paired t-test.

2.13.2. RNA Sequencing

The raw sequencing reads were trimmed with Trim Galore! (http://www.bio-informatics.babra-ham.ac.uk/projects/trim_galore/) (Version 0.3.3), using cutadapt (Version 1.2.1) to remove low-quality bases (quality Phred score cut-off 15) and remaining adaptor sequences. Further information is provided in the Supplemental Experimental Procedures. For all analyses, a p-value (adj.) less than 0.05 was considered as statistically significant and labelled with *, less than 0.01 with **, less than 0.001 with *** and less than 0.0001 with ****.

3. Results

3.1. TWS119 and Rapamycin Induce Phenotypic T_{SCM} Cells

To assess the influence of Wnt and mTOR on human T_{SCM} cell generation, highly purified CD4 + and CD8 + T_N cells (natural (n)) were sorted *ex vivo* (Fig. S1a) and activated with anti-CD3/CD28 beads (1:1 bead/cell ratio) and IL-2 (300 IU/ml) in the presence of the Wnt activator TWS119 (5 μM) or the mTOR inhibitor rapamycin (100 nM).

After 14 days, nCD4 + T_N cells, primed in the presence of TWS119 or rapamycin, formed two lymphocyte populations, a small-sized and a large-sized one, based on forward scatter/side scatter (FSC/SSC) profiles. In contrast, nCD4 + T_N cells which have been cultured in the absence of TWS119 or rapamycin did not generate the small-sized lymphocyte population (Fig. 1a). Phenotypic analysis revealed that the small-sized lymphocyte population mainly consists of T cells with a CCR7 +, CD45RA + T_N-like phenotype and a small fraction of cells with a CCR7 +, CD45RA- T_{CM}-like phenotype. Of note, the T_N-like population displayed phenotypic CD95 +, CD58 + T_{SCM} cells which were significantly increased in absolute cell numbers in comparison to T_{CM}-like cells (Fig. 1b, Fig. S1b and Table 1), suggesting TWS119 and rapamycin as specific inducers of T_{SCM} cells. These cells co-expressed high levels of the CD62L selectin (not shown). We then subdivided the T_N-like population into a CCR7 +, CD45RA^{intermediate} "transition zone" (TZ) and a CCR7 +, CD45RA^{high} "rand zone" (RZ) to investigate whether T_{SCM} cells would be preferentially located in a distinct region of the T_N-like population. Interestingly, this was indeed the case, since the TZ contains higher frequencies of phenotypic T_{SCM} cells compared to the RZ (Fig. 1B), in line with a model of progressive T cell differentiation, positioning T_{SCM} cells in between T_N cells and T_{CM} cells. The large-sized lymphocyte population did not show significant differences in cellular composition upon drug treatment with or without TWS119 or rapamycin and exhibited a mixture of T_N-like, T_{CM}-like and T_{EM}-like (CCR7 −, CD45RA −) cells (Table S1), suggesting the small-sized lymphocyte population as place of CD4 + T_{SCM} cell induction.

To further explore the mechanism of T_{SCM} cell induction by TWS119 and rapamycin, we next tested the alternative Wnt activators Indirubin-3-monoxime (4 μM) and Wnt3A (10 nM) as well as the ATP-competitive mTOR inhibitors PP242 and KU-0063794. PP242 and KU-0063794 used at low concentrations (100 nM) inhibit mTORC1, while at higher concentrations (1 μM) they also block mTORC2 (data not shown). Supporting our finding with rapamycin, 14 days of nCD4 + T_N cell priming in the presence of low-concentrations (100 nM) PP242 or KU-0063794 also triggered the formation of a small-sized lymphocyte population with phenotypic T_{SCM} cells (Fig. 1c and Fig. S1d). However, surprisingly in contrast to TWS119, the alternative Wnt activators Indirubin-3-monoxime and Wnt3A did not generate a small-sized lymphocyte population (Fig. 1c), questioning an involvement of Wnt signalling in T_{SCM} cell induction.

Testing these observations for CD8 + T_{SCM} cell induction, priming of highly purified nCD8 + T_N cells for 14 days in the presence of TWS119 or rapamycin, in comparison to drug absence or priming in the presence of Indirubin-3-monoxime (4 μM), resulted in increased frequencies of T_N-like cells, displaying a population of phenotypic CD95 +, CD58 + T_{SCM} cells (Fig. S1c), suggesting a common pharmacological mechanism of rapamycin and TWS119 also for CD8 + T_{SCM} cell induction. Thus, taken together, inhibitors of mTOR induce phenotypic CD4 + and CD8 + T_{SCM} cells, whereas, apart from TWS119, other Wnt activating drugs fail in doing so.

3.2. TWS119 Inhibits mTORC1

To test the hypothesis about a common pharmacological mechanism of TWS119 and rapamycin in T_{SCM} cell induction, the phosphorylation of GSK-3β (pGSK-3β, read-out for Wnt activity) and the phosphorylation of S6 ribosomal protein (pS6, read-out for mTORC1 activity) were

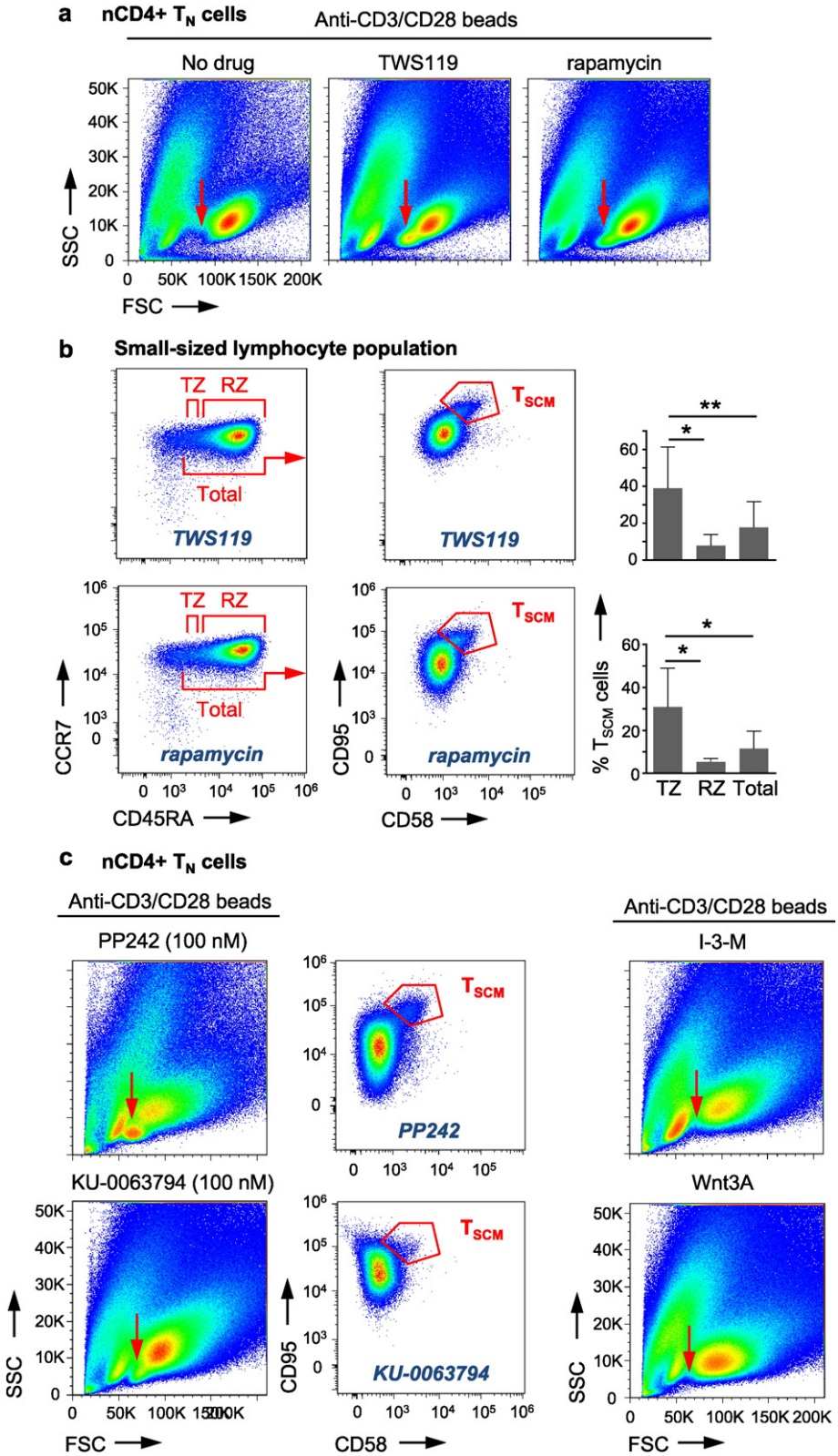

Fig. 1. TWS119 and rapamycin induce phenotypic T_{SCM} cells. (a) Highly purified (T_{SCM} cell-freed) human nCD4+ T_N cells activated for 14 days in the presence of TWS119 (5 μM) or rapamycin (100 nM) form a small-sized lymphocyte population which is not induced in the absence of TWS119 or rapamycin (red arrows). n = 5. (b) The small-sized lymphocyte populations induced by TWS119 or rapamycin mainly consist of CCR7+, CD45RA+ T_N-like cells (gated on live CD3+, CD4+ T cells) and exhibit a fraction of phenotypic CD95+, CD58+ T_{SCM} cells with highest frequencies in the transition zone (TZ). The flow cytometry plot shows phenotypic T_{SCM} cells in the total T_N-like cell population. T_{SCM} cell frequencies are depicted as percentages of the defined zones. Data are represented as mean ± SEM. FSC = forward scatter. SSC = side scatter. RZ = rand zone. T_{SCM} = pharmacologically induced phenotypic T_{SCM} cells. n = 5. (c) Activation of highly purified human nCD4+ T_N cells for 14 days in the presence of PP242 (100 nM) or KU-0063794 (100 nM) also leads to the formation of the small-sized lymphocyte population (red arrows), containing phenotypic CD95+, CD58+ T_{SCM} cells (shown in the total T_N-like cell population). In contrast, priming in the presence of the alternative Wnt activators Indirubin-3-monoxime (I-3-M, 4 μM) or Wnt3A (10 nM) does not lead to the formation of the small-sized lymphocyte population (red arrows). n = 4. T_{SCM} = pharmacologically induced phenotypic T_{SCM} cells.

Table 1
Relative percentages and absolute cell numbers of live CD4 + T_N, T_{SCM} and T_{CM} cells in the small-sized lymphocyte population. Numbers are presented as mean ± standard error of the mean (SEM). n = 5.

	Rapamycin		TWS119	
	%	Absolute	%	Absolute
T_N	86.37 ± 1.02	181.429 ± 19.055	72.36 ± 10.71	120.956 ± 22.647
T_{SCM}	7.97 ± 0.89	16.434 ± 2.175	11.79 ± 2.03	18.312 ± 1.827
T_{CM}	2.54 ± 0.48	5.215 ± 967	5.23 ± 2.46	7.741 ± 3.287

assessed by flow cytometry in highly purified human nCD4 + T_N cells (Fig. 2a) and nCD8 + T_N cells (Fig. 2b) as well as by Western blot analysis for pS6 in highly purified human nCD4 + T_N cells (Fig. 2c) upon activation and drug interference.

Surprisingly, the Wnt activator TWS119, which was able to induce phenotypic T_{SCM} cells, also abolished the phosphorylation of S6 (Fig. 2a to c), suggesting an inhibitory effect of TWS119 on mTORC1. Interestingly, whereas the drugs which inhibited mTORC1 (decrease of S6 phosphorylation) were also capable to induce phenotypic T_{SCM} cells, the drugs which activated Wnt (increase of pGSK-3β) did not induce phenotypic T_{SCM} cells, suggesting that phenotypic T_{SCM} cell induction is mediated by inhibition of mTORC1. In line with reports on differential effects on S6 and 4EBP1 (Choo et al., 2008), TWS119 and rapamycin had no significant effects on p4EBP1, another protein downstream of mTORC1, in nCD4 + T_N cells (Fig. S2a) and nCD8 + T_N cells (Fig. S2b). Moreover, our results suggest that both TWS119 and rapamycin are exerting a mild, suboptimal effect on mTORC1 inhibition (S6K is blocked but 4EBP1 is preserved, as is also mTORC2). Previous studies have demonstrated that S6K is a more sensitive target of mTOR blockade than 4EBP1 (Chresta et al., 2010; Feldman et al., 2009). Thus, inhibition of mTORC1 via decrease of S6 phosphorylation and independence from Wnt signalling emerge as the molecular mechanisms which underlie T_{SCM} cell induction.

3.3. TWS119 Induces a Differentiation Arrest Independently From Wnt Signalling

To confirm this conclusion on a genetic base, we took advantage of highly purified nCD4 + T_N cells from mice with a haematopoietic deletion of β- and γ-catenin, resulting in abolished Wnt signalling. In mice, T_{SCM} cells were phenotypically defined by the expression of Sca-1 (Ly6A/E) and CXC chemokine receptor 3 (CXCR3) on naive-appearing CD44 −, CD62L + T cells (Fig. S3a) (Gattinoni et al., 2009; Zhang et al., 2005). Since mouse nCD4 + T_N cells did not tolerate long drug treatment phases, we needed to reduce priming periods to 4 days with 1.5 μM TWS119, an interval possibly too short to trigger an up-regulation of T_{SCM} cell markers. However, to confirm its independence from Wnt signalling, we hypothesised that under these conditions TWS119 would at least arrest a fraction of activated β- and γ-catenin KO nCD4 + T_N cells in a T_N-like state, in analogy to the formation of the small-sized lymphocyte population observed in the *in vitro* experiments with human nCD4 + T_N cells. Interestingly, as observed for the mTORC1 inhibitor rapamycin, this was also indeed the case for TWS119, whereas the alternative Wnt activator SB216763 (2 μM), which does not inhibit mTORC1, failed in doing so (Fig. 3 and Fig. 2c). Thus, these data further confirm that the mediation of a differentiation arrest, as prerequisite for T_{SCM} cell induction, is independent from Wnt signalling, but dependent on mTORC1 inhibition. To further corroborate these findings, we then assessed T_{SCM} cell levels in the spleens of β- and γ-catenin KO mice, using the above mentioned phenotype. Suggesting no impairment in T_{SCM} cell generation in the absence of Wnt signalling, β- and γ-catenin KO mice exhibited naturally occurring T_{SCM} cells in comparable frequencies as their WT counterparts (Fig. S3b). Furthermore, we took advantage of mice with a T cell-specific KO of the mTORC1 regulatory component Raptor, which leads to an abolishment of mTORC1 signalling. Interestingly, supporting our *in vitro* findings of rapamycin-mediated T_{SCM} cell induction, we found significantly increased T_{SCM} cell frequencies in these mice (Fig. S3c and Fig. S3d). Moreover, excluding an off-target effect of rapamycin, additional treatment of Raptor KO nCD4 + T_N cells during 4-day priming with rapamycin (100 nM) did not result in an increased fraction of cells in a T_N-like state (Fig. S3e). Altogether, these data present further evidence for the inhibition of mTORC1 as the molecular mechanism underlying T_{SCM} cell induction.

3.4. Transcriptome Analysis of Naturally Occurring and Pharmacologically Induced T_{SCM} Cells

By transcriptome analysis, we next set out to assess the degree of relatedness between naturally occurring CD4 + T_N, T_{SCM} and T_{CM} cells as well as TWS119- and rapamycin-induced CD4 + T_{SCM} cells to gain insights into distinct profiles of gene expression in CD4 + T_{SCM} cells. In naturally occurring T cell subsets, unsupervised analysis showed a very close relatedness between T_{SCM} and T_{CM} cells compared to T_N cells (Fig. 4a and b), potentially indicating a continuous transition from T_{SCM} to T_{CM} cells during differentiation. Suggesting CD4 + T cell differentiation as process which may be strictly regulated by a core set of genes, only 895 genes were found to be significantly differentially expressed between T_N and T_{SCM} cells and 141 genes between T_{SCM} and T_{CM} cells by supervised analysis (adj. $p < 0.05$; $|\log2FC| > 1$) (Fig. 4c, Table S2, Table S3). To identify further differences between T_{SCM} and T_{CM} cells with respect to the stem cell-like nature of T_{SCM} cells, we carried out a gene set enrichment analysis for stem cell characteristic genes (view Supplemental Information) and could identify *FGFR1*, *RB1* and *NOTCH2* to be highly expressed in T_{SCM} cells in comparison to T_{CM} cells (adj. $p = 0.07$). Of further interest for the distinction of T_{SCM} from T_{CM} cells, 18 genes were found to be significantly differentially expressed between these otherwise closely related subsets and not shared by any other subset (Fig. 4c and Table 4). In addition, a set of 56 genes could be identified to be significantly differentially expressed between T_N and T_{SCM} cells and between T_{SCM} and T_{CM} cells, thus, showing a unique expression profile in T_{SCM} cells (Fig. 4c and Table 2). Interestingly, from these 56 genes only 4 genes, *SLC22A17*, *RAI2*, *SALL2* and *LOC338651*, were down-regulated in T_{SCM} cells (Fig. S4a), whereas all the other genes were up-regulated. Moreover, with exception of *TCF4*, Wnt signalling transducers could be found to be highly expressed either in both, T_N and T_{SCM}, or significantly up-regulated in T_N cells, further arguing against the theory that activation of the Wnt pathway in T_N cells induces T_{SCM} cells (Fig. S4b).

Interestingly, TWS119- and rapamycin-induced T_{SCM} cells showed a very close degree of relatedness. From 21,481 interrogated genes, only 565 genes were significantly differentially expressed between them (adj. $p < 0.05$; $|\log2FC| > 1$), further supporting our finding of a common pharmacological mechanism of these drugs (Fig. 4a to c and Table S5). However, since TWS119- and rapamycin-induced T_{SCM} cells have received strong activating stimuli over 14 days, it was likely that their transcriptome differed from the ones of naturally occurring T_{SCM} cells, directly sorted *ex vivo* in their resting state. Nonetheless, we hypothesised that the set of well-known factors of human effector and memory T cell differentiation would show a comparable expression profile in naturally occurring and pharmacologically induced T_{SCM} cells (Gattinoni et al., 2011). Indeed, similar expression levels of the regulators of effector differentiation *CXCR3*, *KLRG1*, *PRDM1* and *TBX21* could be found (Fig. 4d). Interestingly, *in vitro* induced T_{SCM} cells exhibited higher expression levels of *GZMA* and *PRF1* (Fig. 4d), probably equipping them with superior direct effector functions. *In vitro* induced and naturally occurring T_{SCM} cells displayed a similar expression level of *TNF*, but, notably, *in vitro* induced T_{SCM} cells exhibited low *IFNG* expression levels (Fig. S4c). This might be a result of *IFNG* down-regulation due to mTORC1 inhibition, a mechanism described for type I interferons in plasmacytoid dendritic cells mediated

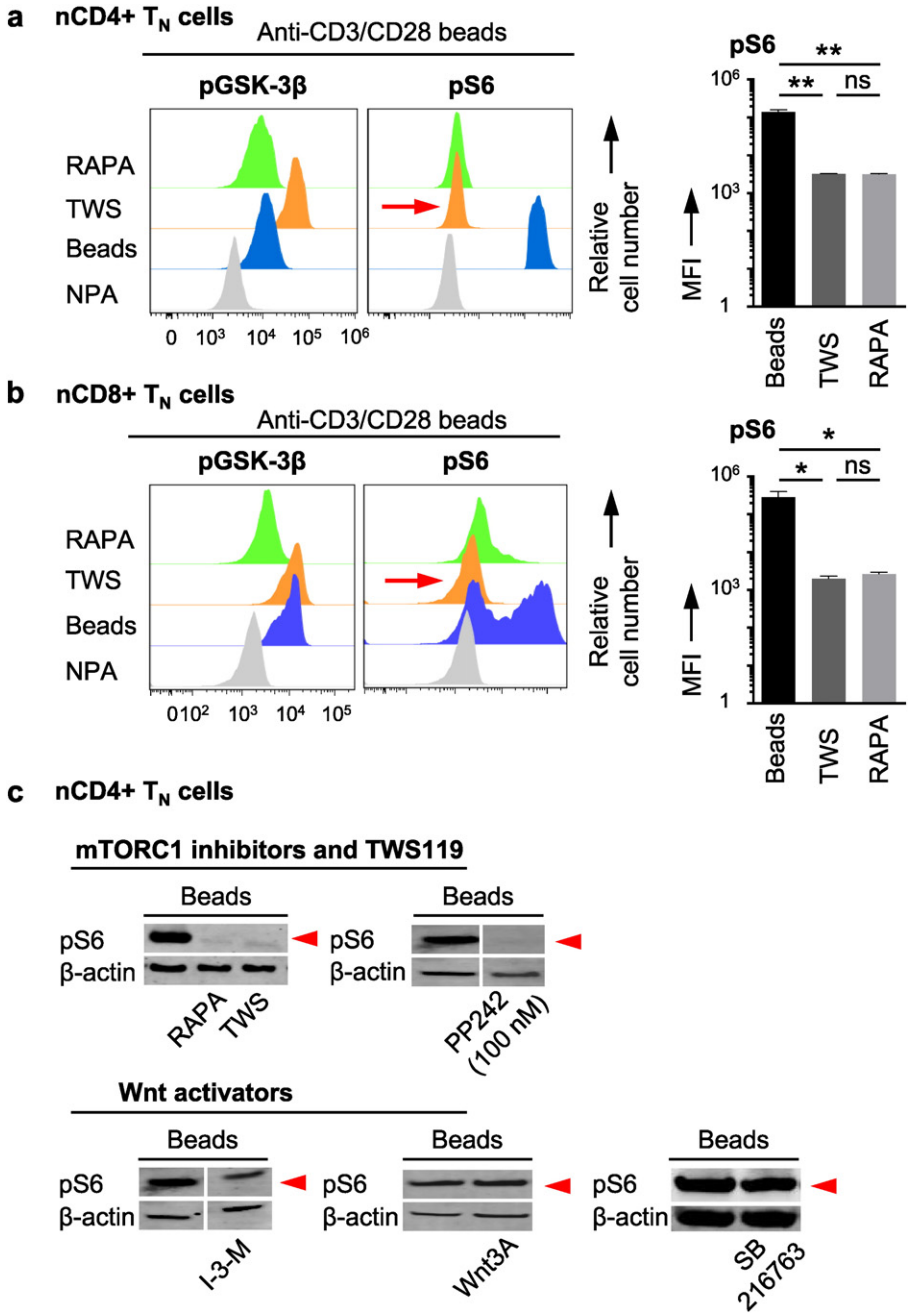

Fig. 2. TWS119 inhibits mTORC1. Assessment of phosphorylation of GSK-3β (Ser9) and of phosphorylation of S6 ribosomal protein (Ser235/236) by flow cytometry in (a) highly purified (T_{SCM} cell-freed) nCD4+ T_N cells and in (b) highly purified nCD8+ T_N cells. n = 3. (c) Assessment of phosphorylation of S6 ribosomal protein (Ser235/236) by Western blot technique in highly purified nCD4+ T_N cells. n = 3. Activation of T_N cells in the presence of rapamycin (100 nM), PP242 (100 nM) and, of note, also of the Wnt activator TWS119 (5 μM) inhibits mTORC1 signalling. In contrast, the alternative Wnt activators Indirubin-3-monoxime (I-3-M, 4 μM), Wnt3A (10 nM) and SB216763 (4 μM) do not reduce phosphorylation of S6. NPA = no primary antibody. Beads = Anti-CD3/CD28 beads. TWS = TWS119. RAPA = rapamycin. MFI = median fluorescence intensity.

by interferon-regulatory factor (IRF) 7 (Cao et al., 2008). Interestingly, IRFs are involved in CD4+ T cell differentiation (Lohoff and Mak, 2005), and *IRF7* was found to be up-regulated in *in vitro* induced T_{SCM} cells (Fig. S4c). Furthermore, similar expression levels of the inhibitory factors for T cell activation and differentiation *CERS6*, *EOMES*, *LEF1*, *TAF4B* and *ACTN1* as well as for the T_{SCM} cell characteristic factors *CD27*, *ITGAL*, *IL2RB* and *TNFSF9* could be identified (Fig. 4d). In addition, the expression levels of genes encoding distinct interleukins are shown in Fig. S4d. Finally, confirming the purity of the performed cell sorts, naturally occurring T_N, T_{SCM} and *in vitro* induced T_{SCM} cells expressed similarly low amounts of *HNRPLL*, a key regulator of the alternative splicing of the *CD45* pre-mRNA (Oberdoerffer et al., 2008). Additionally, *FAS* was among the most significantly differentially expressed genes between naturally occurring T_N and T_{SCM} cells (Fig. S4e). Altogether, these data present insights into the transcriptional regulation of T_{SCM} cells and underline the pharmacological inhibition of mTORC1 as a molecular mechanism to confer stemness to a population of activated T_N cells.

3.5. In Vitro Induced T_{SCM} Cells Exhibit a Long-term Repopulation Capacity in Vivo

The distinct up-regulation of transcripts encoding telomerase, anti-apoptotic genes and positive cell cycle regulators and down-regulation of pro-apoptotic genes and CDK inhibitors (Fig. S5a) (Igney and Krammer, 2002; Vermeulen et al., 2003) suggested that *in vitro* induced

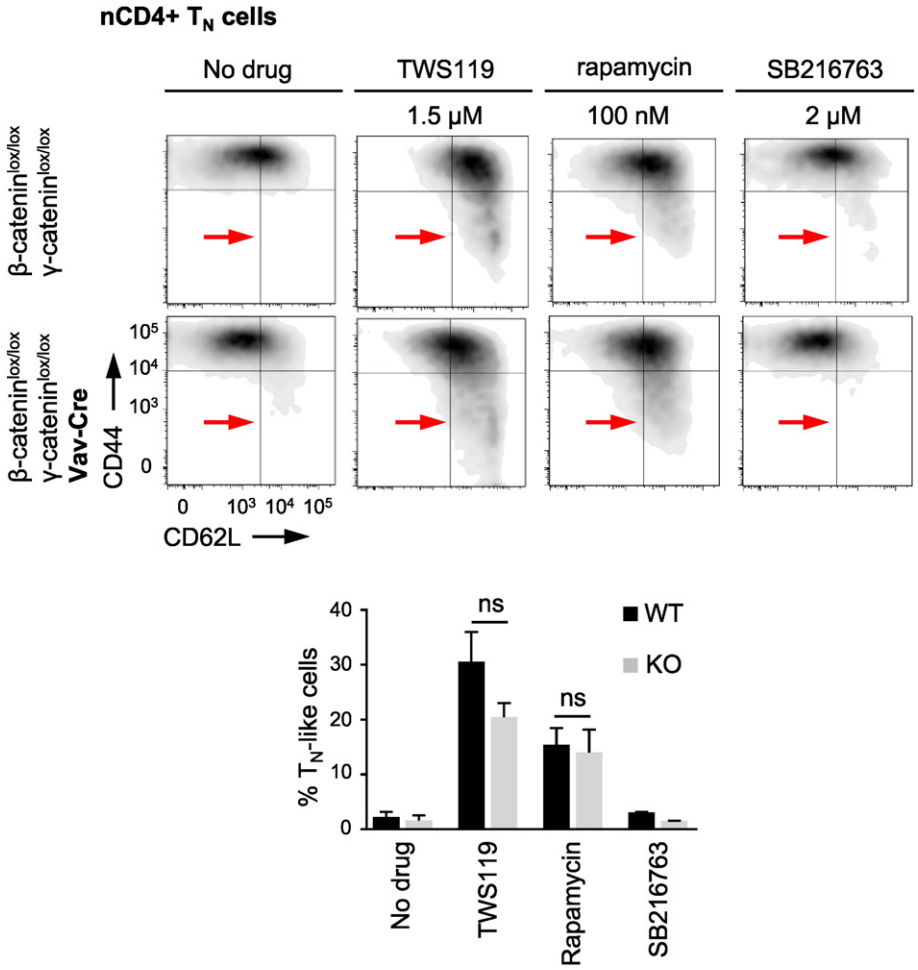

Fig. 3. TWS119 acts independently from Wnt. Both, TWS119 (1.5 μM) and rapamycin (100 nM), arrest a fraction of highly purified (T_{SCM} cell-freed) wild-type (WT, β-catenin$^{lox/lox}$ γ-catenin$^{lox/lox}$, top) and β- and γ-catenin knockout (KO, β-catenin$^{lox/lox}$ γ-catenin$^{lox/lox}$vav-cre, bottom) nCD4+ T_N cells after 4 days of *in vitro* activation with anti-CD3 (2 μg/ml), anti-CD28 antibody (2 μg/ml) and IL-2 (10 ng/ml). In contrast, SB216763 (2 μM) fails to mediate this differentiation arrest in activated WT and KO nCD4+ T_N cells. T_N-like cell frequencies are depicted as percentages of live CD3+, CD4+ T cells. n = 3. Data are represented as mean ± SEM. ns = not significant.

CD4+ T_{SCM} cells might exhibit a superior *in vivo* long-term persistence. We directly assessed this potential *in vivo* long-term persistence by adoptive transfer of 200,000 rapamycin-induced CD4+ T_{SCM} cells, isolated to high purity by flow cytometry-based cell sorting, into NOD.Cg-Prkdc^{scid}Il2rg^{tm1Wjl}/SzJ (NSG) mice. Ten weeks after adoptive transfer, peripheral blood, spleen, bone marrow, lung and liver were investigated by multicolour flow cytometry for T_{SCM} cell persistence (Fig. 5a and Fig. S5b). Interestingly, in two of three experiments, the spleens of the mice, which have received T_{SCM} cells, showed the presence of a live CD3+, CD4+ T cell population with a CCR7−, CD45RA-^{intermediate} phenotype (Fig. 5a), indicating both, the potential of *in vitro* induced CD4+ T_{SCM} cells to persist long-term *in vivo* and their ability to repopulate the effector pools by giving rise to further differentiated progeny. In a third experiment, adoptively transferred T_{SCM} cells yielded live CD3+, CD4+ T cells in the peripheral blood ten weeks after adoptive transfer (Fig. 5a). In contrast, no T cells could be detected after adoptive transfer of same numbers of T_N-like or T_{CM}-like cells, re-sorted from the small-sized lymphocyte population from the same *in vitro* cell culture (Fig. S5b). Spleen size and weight did not exhibit any differences between the groups (Fig. S5b). Of note, compared to naturally occurring CD4+ T_N cells, *in vitro* induced CD4+ T_{SCM} cells showed an up-regulation of the haematopoietic stem cell engraftment genes *HOXA1* and *LPXN* (Powers and Trobridge, 2013), which might have mediated their superior engraftment capacity (Fig. S5c). Together, these data suggest a potential advantage of pharmacologically induced CD4+ T_{SCM} cells in mediating a prolonged immune response after adoptive transfer. Of note, we did not observe signs of xeno-GVHD in contrast to a report showing that rapamycin-treated T cells caused more xeno-GVHD (Amarnath et al., 2010). Further studies are warranted to assess the relative functional features of rapamycin-induced T_{SCM} cells and their long-term repopulation capacity after adoptive transfer.

Next, the proliferative capacity of 30,000 rapamycin-induced CD4+ T_{SCM} cells in comparison to equal numbers of T_N-like and T_{CM}-like cells, re-sorted from the small-sized lymphocyte population from the same *in vitro* cell culture, was assessed by CFSE dilution assay. T cells were either left for 6 days in presence of IL-2 (50 IU/ml) or, additionally, stimulated with OKT3 (1 μg/ml) and anti-CD28 antibody (10 μg/ml) (Fig. 5b). Interestingly, in two of six experiments, stimulated *in vitro* induced T_{SCM} cells formed a small-sized resting T cell population in addition to a large proliferating one, probably reflecting their stem cell nature, which is both, the capacity to self-renew and to differentiate (Fig. 5b).

3.6. Substrate Utilization and Cellular Metabolism of T_{SCM} Cells

Increasing evidence suggests that T cell differentiation is controlled by fine-tuned modulations of glycolysis and fatty acid oxidation (FAO) (Cham et al., 2008; Fox et al., 2005; Zheng et al., 2009). To investigate the predominance of a distinct metabolic programme in T_{SCM} cells, we next measured the uptake capacity of the fluorescent glucose analogue

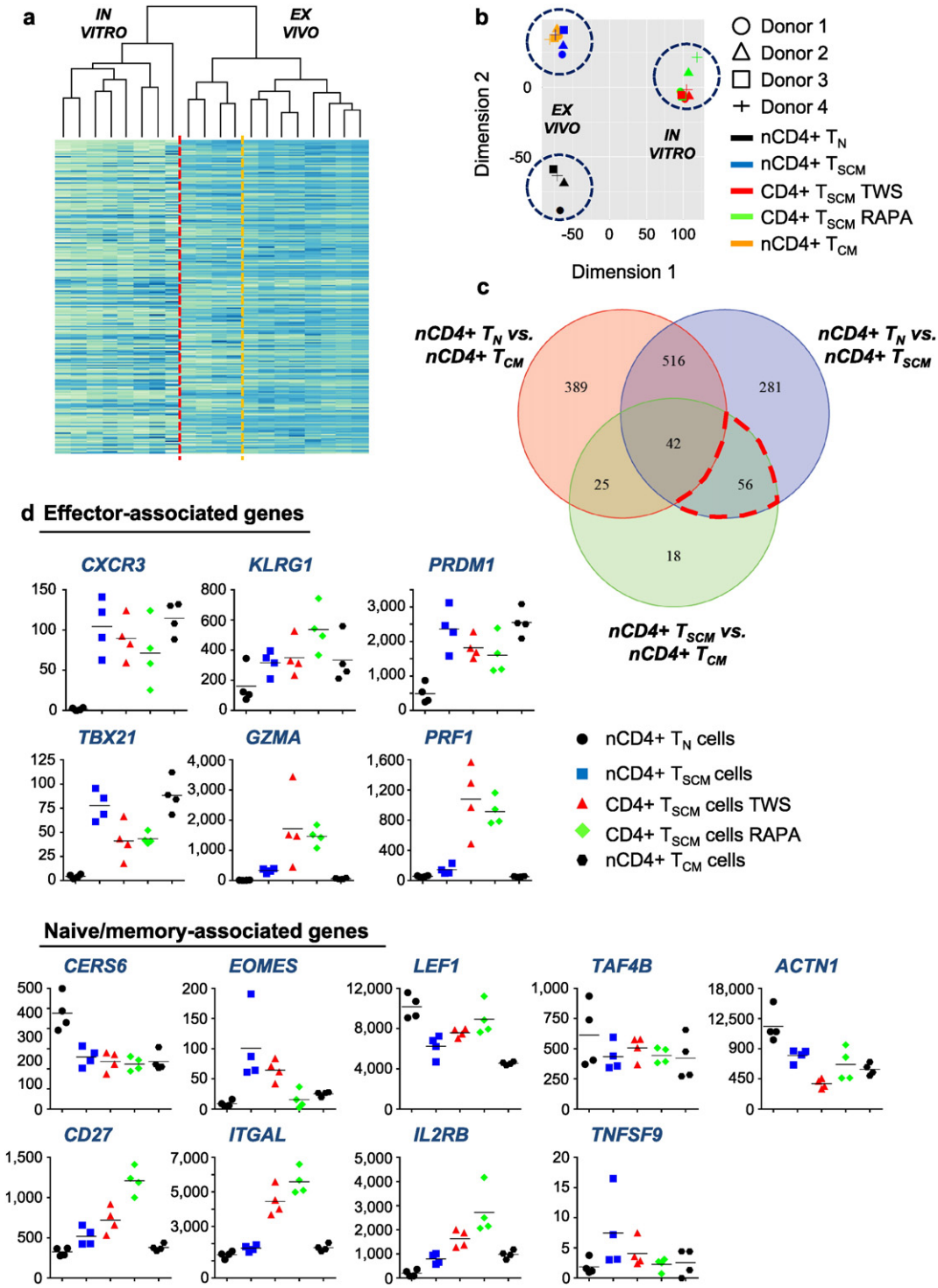

Fig. 4. Fate-determining key factors in naturally occurring and pharmacologically induced T_{SCM} cells. Heat map of gene expression among nCD4 + T_N cells, T_{SCM} cells and T_{CM} cells as well as TWS119- and rapamycin-induced CD4 + T_{SCM} cells. For interpretability, only the 1000 genes with the highest average normalized count levels across all samples were included in the heat map (Table S6). (b) Principal component analysis led to grouping of naturally occurring T cells on the one side and pharmacologically induced T cells on the other side by the first two principal components. In the first group, T_{SCM} cells and T_{CM} cells are most similar to each other. The first principle component captured a large fraction (35.5%) of the total variance in the data. (c) Venn diagram depicting overlaps among significantly differentially expressed genes found in pairwise comparisons between T_N cells, T_{SCM} cells and T_{CM} cells. Numbers indicate genes. The set of 56 genes is circled in red. (d) Comparative graphic representation of expression levels of naive/memory- and effector-associated genes in T_N cells, T_{SCM} cells, T_{CM} cells and TWS119- and rapamycin-induced T_{SCM} cells. The y-axes show normalized counts. Data are based on transcriptome analysis in 4 healthy human individuals. D1–4 = Donor 1–4. T_N = T_N cells. T_{SCM} = T_{SCM} cells. T_{CM} = T_{CM} cells. TWS = TWS119-induced T_{SCM} cells. RAPA = rapamycin-induced T_{SCM} cells.

2-NBDG in rapamycin-induced T_{SCM} cells in comparison to T_N-like, T_{CM}-like and T_{EM}-like cells and to the respective naturally occurring T cell subsets as reference point for glycolytic activity (Sukumar et al., 2013b). Interestingly, compared to the divergent glucose uptake of T_{EM} cells and T_{EM}-like cells, all other T cell subsets exhibited a limited glucose uptake, suggesting especially for T_{SCM} cells an independence from glycolysis (Fig. 5c). In line, pharmacologically induced T_{SCM} cells also showed low expression of the gene encoding the master regulator

Table 2
56 genes shared between the sets of genes found to be differentially expressed between the nCD4 + T_N cell and nCD4 + T_{SCM} cell groups as well as between the nCD4 + T_{SCM} cell and nCD4 + T_{CM} cell groups, but not between the nCD4 + T_N cell and nCD4 + T_{CM} cell groups.

Gene name
1. IKZF4
2. SWAP70
3. FAM49A
4. HLA-DPB1
5. COBLL1
6. FCRL1
7. FCER1G
8. HBA1
9. SELP
10. HLA-DMB
11. CCL4
12. IFI30
13. IGLL5
14. BTK
15. LAYN
16. HLA-DMA
17. PTPN3
18. NKG7
19. WDFY4
20. PHACTR1
21. ANKRD33B
22. CDK14
23. COL19A1
24. CCL3
25. FAM129C
26. TLR5
27. SERPINA1
28. GFOD1
29. ARHGAP24
30. BANK1
31. ADAM12
32. GZMB
33. ARAP3
34. SLC22A17
35. IGJ
36. RAI2
37. TYROBP
38. PRF1
39. CAV1
40. FHL3
41. CNR2
42. LOC100130357
43. SALL2
44. KIAA0226L
45. CYBB
46. CD22
47. MNDA
48. MT1L
49. ALAS2
50. LYN
51. FCRL2
52. MS4A1
53. LOC338651
54. SNCA
55. SETBP1
56. HBG2

of glycolytic enzyme *HIFA* (Fig. S5d). Alternatively, as reference point for oxidative metabolism such as FAO, we measured the mitochondrial membrane potential (MMP) in the mentioned T cell subsets by assessment of their uptake of TMRE, a dye, which accumulates in active mitochondria of short-lived effectors (Sukumar et al., 2013a). Accordingly, we could find an increase of TMRE uptake going along with progressive cellular differentiation (Fig. 5d).

Since these observations suggest that T_{SCM} cells rather gain their energy from an oxidative metabolism, we hypothesised that FAO might also be the relevant metabolic programme in the induction of T_{SCM} cells. We, therefore, investigated the impact of the pharmacological T_{SCM} cell inducers TWS119 and rapamycin on the metabolism of activated nCD4 + T_N cells by assessment of ECAR, which is an indicator of glycolytic activity, and OCR, which is an indicator of mitochondrial respiration, by Seahorse analysis (Fig. 5e left). Interestingly, administration of TWS119 (5 μM) or rapamycin (100 nM) prevented the development of full cellular glycolytic activity in response to oligomycin (1 μg/ml), a drug, enforcing maximal glycolysis. Thus, we hypothesised that TWS119 and rapamycin initiate a metabolic programme for T_{SCM} cell induction which is alternative to glycolysis. To disclose whether this metabolic programme would be FAO, we triggered mitochondrial respiration in rapamycin-pretreated (100 nM, 2 h) and activated nCD4 + T_N cells by administration of palmitate (500 μM), the ester of retinol and palmitic acid. Interestingly, the presence of palmitate increased mitochondrial respiration to the levels measured in nCD4 + T_{SCM} cells (Fig. 5e right). Thus, these data present evidence for FAO as metabolic programme characteristic of T_{SCM} cells and needed for T_{SCM} cell induction.

4. Discussion

The identification of the signalling pathways, underlying T_{SCM} cell formation, allows their targeted induction and paves the way for the design of novel immunotherapeutic approaches. Here, we show the emergence of a T cell population with phenotypic, transcriptional, functional and metabolic hallmarks of naturally occurring T_{SCM} cells upon *in vitro* inhibition of mTORC1 during priming of human T_N cells. These findings emphasize the potential relevance of the signalling network of mTOR kinase in immunotherapy and of mTOR modulating pharmacological agents.

Interestingly, we show that mTORC1 inhibition with drugs like rapamycin mediates an immunostimulatory effect by the induction of T_{SCM} cells, although these drugs are generally used because of their immunosuppressive function (Cobbold, 2013; Ferrer et al., 2011). Thus, these observations indicate that there are distinct conditions which trigger either a preferential immunostimulatory or an immunosuppressive rapamycin effect. Among a variety of different molecular mechanisms, rapamycin has been suggested to fulfil its immunosuppressive function by prevention of full T cell activation (Loewith et al., 2002; Thomson et al., 2009). This effect can be circumvented by strong stimulation of the TCR and co-stimulatory receptors (Slavik et al., 2004). Similarly, in the *in vitro* experiments the high degree of activation of T_N cells by anti-CD3/CD28 beads in a 1:1 bead/cell ratio and 300 IU/ml IL-2 might have favoured an immunostimulatory rapamycin effect. Furthermore, rapamycin has been shown to increase the antigen-specific T cell response to a pathogen (short-term persistence of the antigen), but to fail in doing so in response to a graft (long-term persistence of the antigen) (Ferrer et al., 2010). These findings strongly suggest that the period of antigen persistence also regulates the immunological outcome of rapamycin. Thus, the rather short periods of T_N cell activation (14 days and 4 days) in our *in vitro* experiments might have tipped the balance towards an immunostimulatory rapamycin effect. The used concentration of rapamycin also emerges as an important factor for mediating either an immunostimulatory or an immunosuppressive drug effect. For the *in vitro* induction of T_{SCM} cells, rapamycin was used in 100 nM (90 ng/ml), since a rather high concentration of 40–100 ng/ml rapamycin, administered during the contraction phase, has been shown to qualitatively improve antigen-specific memory T cells in a mouse model of CD8 + T cell response to acute viral infection (Araki et al., 2009). In contrast, 8–12 ng/ml rapamycin blood levels are intended to induce immunosuppression after transplantation (Baan et al., 2005). Together, this suggests that a low rapamycin concentration preferentially results in an immunosuppressive effect, whereas a high rapamycin concentration triggers an immunostimulatory one. Also the immunomodulatory actions of rapamycin might be regulated by the interplay between the two mTOR complexes. Whereas T_{SCM} cell induction, as shown here, follows mTORC1 inhibition without additional

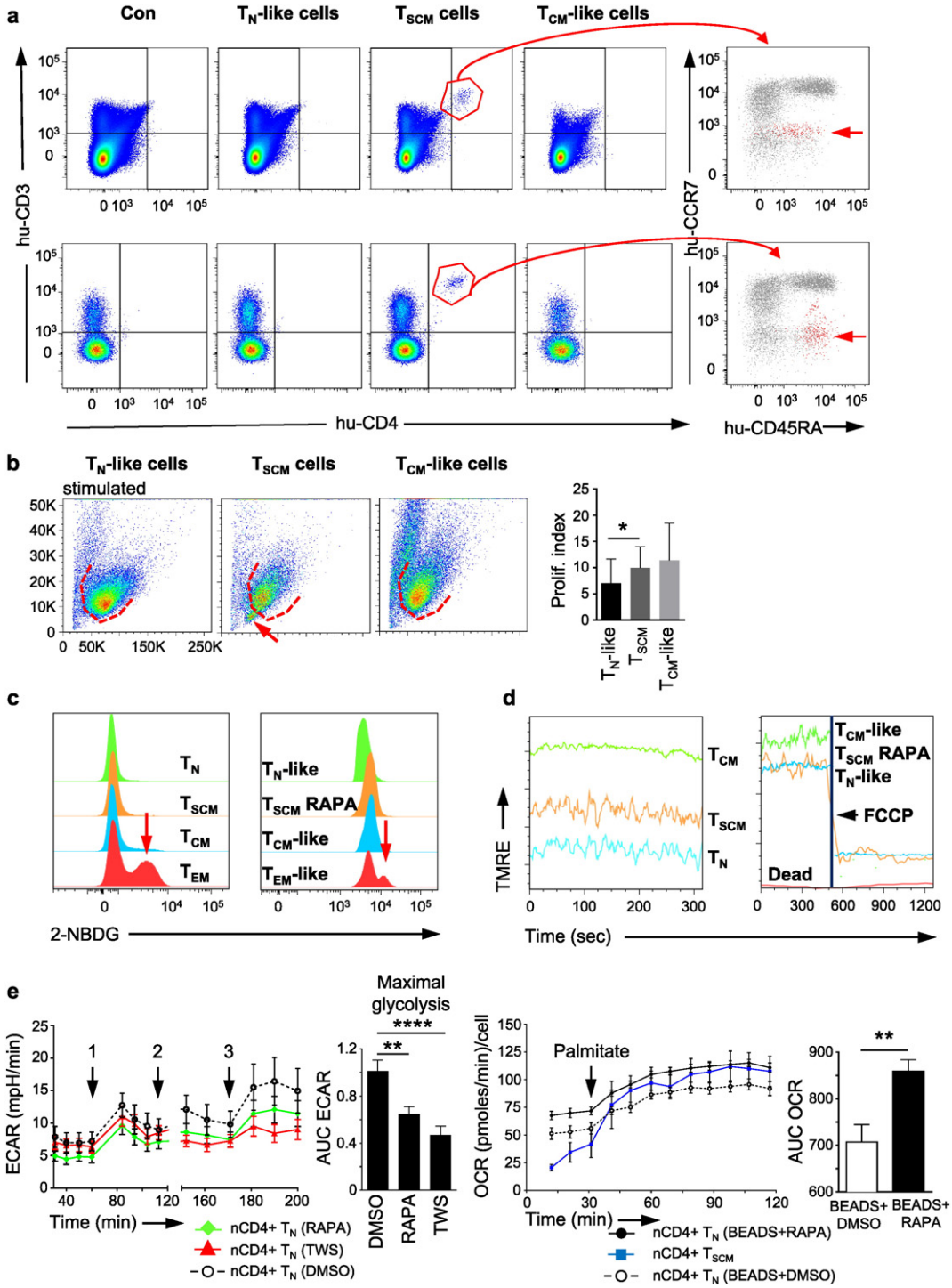

Fig. 5. *In vivo* long-term repopulation capacity and cellular metabolism of CD4+ T_{SCM} cells. (a) Live CD3+, CD4+ T cells with a CCR7−, CD45RA intermediate phenotype can be detected in the spleen and peripheral blood of NSG mice, ten weeks after adoptive transfer of 200,000 rapamycin-induced CD4+ T_{SCM} cells. Con = control: injection of 200 μl culture medium. The grey underlay shows the distribution of CCR7 and CD45RA expression in live CD3+, CD4+ T cells in a healthy donor control. n = 3. (b) Rapamycin-induced CD4+ T_{SCM} cells show a proliferative profile similar to the one of T_{CM}-like cells. In two of six experiments, activated rapamycin-induced CD4+ T_{SCM} cells formed an additional small-sized lymphocyte population, which resisted to activating stimuli (red arrow). n = 6. (c) CD4+ T_{EM} and T_{EM}-like cells display a divergent glucose uptake capacity. In comparison, nCD4+ T_N, T_{SCM} and T_{CM} cells as well as rapamycin-induced CD4+ T_{SCM}, T_N-like and T_{CM}-like cells do not show high 2-NBDG incorporation. n = 3. (d) Increase of mitochondrial membrane potential (MMP), measured by TMRE uptake, goes along with progressive T cell differentiation. Administration of the oxidative decoupler FCCP leads to immediate MMP breakdown, proving the T cells` viability. n = 3. (e) Top: Activation of nCD4+ T_N cells with anti-CD3/CD28 beads increases ECAR (1). Administration of TWS119 (5 μM) or rapamycin (100 nM) (2) hinders activated T_N cells to fully develop glycolytic activity upon oligomycin (1 μg/ml) injection (3). n = 4. Bottom: Palmitate (500 μM) substitution increases the OCR in rapamycin-pre-treated, activated T_N cells to similar levels as the ones of nCD4+ T_{SCM} cells. n = 3. Data are represented as mean ± SEM. ECAR = extracellular acidification rate. OCR = oxygen consumption rate. AUC = area under the curve. T_N = T_N cells. T_{SCM} = T_{SCM} cells. T_{CM} = T_{CM} cells. T_{EM} = T_{EM} cells. T_N-like = T_N-like cells. T_{CM}-like = T_{CM}-like cells. T_{SCM} RAPA = rapamycin-induced T_{SCM} cells. RAPA = rapamycin. TWS = TWS119. BEADS = anti-CD3/CD28 beads.

inhibition of mTORC2, formation of immunosuppressive regulatory T cells is favoured in additional absence of mTORC2 signalling (Chi, 2012). Thus, immunomodulation by rapamycin appears to be a fine-tuned, highly multidimensional process.

Furthermore, we show that the induction of T_{SCM} cells is completely independent from the Wnt signalling pathway. In line with this, the role of Wnt in memory T cell formation has already been called into question by reports about memory T cell formation in CD8 + T cells, in which β-catenin was conditionally knocked out (Driessens et al., 2010; Prlic and Bevan, 2011). Nevertheless, these reports have to be seen with caution, since, in contrast to our study, specifically, T_{SCM} cell formation was not investigated and mice with KO of only β-catenin, which might have favoured a bypassed activity of Wnt signalling by γ-catenin, were used. Moreover, our data offer an unexpected answer to the paradox finding that the Wnt activator TWS119 induces T_{SCM} cells, whereas none of alternative Wnt activators was able to do so, by the discovery of an mTORC1 inhibiting effect of TWS119. Interestingly, this effect finds further confirmation by a recent report, confirming in mouse T cells that TWS119 inhibits mTORC1 (Xiao et al., 2013). At present, it is unclear what the scope of TWS119 off-target effects on other kinases is or whether its inhibition of the mTORC1 kinase requires, as rapamycin, FKBP12. Future biochemical and pharmacological studies will have to address the precise molecular mechanism of mTORC1 inhibition by TWS119.

We also showed that mTORC1 inhibition switched the metabolic programme of activated nCD4 + T_N cells to an oxidative metabolism dependent on FAO. However, prominently, in the *in vitro* experiments only a fraction of activated T_N cells was arrested in a T_N-like state by TWS119 or rapamycin, suggesting that not all T_N cells from the phenotypically homogenous CCR7 +, CD45RA + starting population react to mTORC1 inhibition in the same way. Future studies will have to address whether T_N cell intrinsic factors can be identified which predispose certain cells to stop differentiation upon mTORC1 inhibition. One such factor might be Krüppel-like-factor 2 (KLF2) which has been shown to maintain the expression of CCR7 and CD62L and has been suggested to be up-regulated upon mTORC1 inhibition (Chi, 2012; van der Windt et al., 2012). Interestingly, only a small fraction of the CCR7 +, CD45RA +, nCD4 + T_N cell starting pool exhibited a high KLF2 expression, whereas the vast majority showed a low expression of KLF2 (Fig. S5e), suggesting KLF2 as possible discriminator to delineate T_N cells with T_{SCM} cell precursor potential.

We sought to compare the transcriptome of CD4 + T_{SCM} cells induced by either TWS119 or rapamycin. Indeed, we observed a very highly overlapping gene expression signature shared by rapamycin- and TWS119-induced CD4 + T_{SCM} cells. Among 21,481 interrogated genes, only 565 genes were significantly differentially expressed between them (adj. $p < 0.05$; $|\log2FC| > 1$), further supporting a common pharmacological mechanism of these drugs. It is very interesting that several of the up-regulated genes in the rapamycin treatment group were related with cell metabolism (Supplemental Table 5). Of note, the most highly up-regulated gene with rapamycin induction is NAD(P)H:quinone oxidoreductase (NQO1), which protects cells against oxidative stress and toxic quinones. In line with this, TXNRD1 (encoding the thioredoxin reductase 1) was also up-regulated in rapamycin-induced T_{SCM} cells. This protein could reduce thioredoxins and plays an important role in protection against oxidative stress. High expression of NQO1 and TXNRD1 might be closely related with the increased oxidative phosphorylation and fatty acid oxidation upon rapamycin induction of T_{SCM}, which definitely needs to be addressed further. On the other hand, the most up-regulated gene in TWS119-induced T_{SCM} cells is LAMP3 (CD63). CD63 is barely expressed in naïve T cells but induced upon T cell activation. Crosslinking of CD63 has been shown to deliver a potent co-stimulatory signal to T cells. To our surprise, we noticed a striking induction of interferon responsive gene expression pattern in TWS119-induced T_{SCM} cells (for example, interferon-induced protein with tetratricopeptide repeats 2, IFIT2; Interferon-Induced Protein with Tetratricopeptide Repeats 3, IFIT3; interferon alpha-inducible proteins 6, IFI6; interferon alpha-inducible proteins 27, IFI27). Many of these genes have been shown to be important for antiviral innate immunity. Some of them emerge to play important roles in regulating T cell activation and immune response. For instance, ISG15 protease UBP43 (USP18) regulates T cell activation. USP18 deficient T cells exhibit hyperactivation of NF-κB and NFAT upon TCR triggering and are defective in Th17 differentiation. The roles of many of those genes in regulating T cells immunity remain to be determined in the near future.

From a translational standpoint, T_{SCM} cells emerge as most promising population for immunotherapy. In this regard, recent reports which indicate that the efficacy of CAR T cells might be based on their acquisition of a T_{SCM} cell phenotype are highly encouraging (Yang et al., 2014); however, previous work showed that also other T cell populations have the capacity to persist long-term *in vivo* (Berger et al., 2008; Markley and Sadelain, 2010). Our data suggest the use of rapamycin for efficient *in vitro* T_{SCM} cell induction or *in vivo* application to enrich for antigen-specific T_{SCM} cells, which should be performed over a short period and by high drug concentration. However, the latter approach will need clinical studies titrating rapamycin doses and assessing different application time-points. Also our insights into T_{SCM} cell metabolism could be used for clinical purposes, since it seems to be rational to provide glucose in treatment phases in which a strong immune attack by T_{EFF} cells is desired. In contrast, in periods of long-term tumour control, in which T cells should enter low differentiation states, substrates allowing FAO should be unrestrictedly provided. In addition, future studies will have to assess the characteristics of and interplay between naturally occurring CD8 + T_{SCM} cells and CD4 + T_{SCM} cells as well as their rapamycin- and TWS119-induced counterparts in preclinical and clinical *in vivo* settings.

Thus, cellular signalling and metabolism emerge as most promising targets to influence T_{SCM} cell differentiation for the design of innovative immunotherapies.

Conflicts of Interest

The authors declare no conflicts of interest.

Author Contributions

G.S. designed the study, performed the experiments and wrote the manuscript. C.J. designed the study, performed *in vitro* experiments and wrote the manuscript. L.Z. performed *in vivo* experiments and wrote the manuscript. C.G. performed experiments with β-/γ-catenin KO mice. IC.L-M. carried out metabolic analysis. C.S. performed statistical data analysis. M.D. provided critical input in statistical data analysis. W.H. provided critical input in experimental design. L.F. provided critical input in the assessment of cellular metabolism. O.D. designed the study. P.R. designed and supervised the study, wrote the manuscript, provided critical input, set up collaborations and secured material funding.

Acknowledgements

This study was supported by a grant from the German Research Foundation: *Scholz, G (2012): The role of Wnt and mTOR in human memory T cell differentiation*. The authors sincerely thank Danny Labes (Flow Cytometry Facility, UNIL) for his input in technical issues and assistance in data acquisition and analysis. The authors also thank Keith Harshman and his team (Genomic Technologies Facility, Center for Integrative Genomics, UNIL) for the professional collaboration in RNA sequencing. The authors also sincerely thank Glenn L. Radice (Department of Medicine, Thomas Jefferson University, Philadelphia, Pennsylvania, USA) and Eliane J. Müller (Vetsuisse Faculty, University of Bern, Bern, Switzerland) for providing conditional γ-catenin KO mice. C.J. was funded in part by a Marie Heim-Vögtlin grant from the Swiss

National Science Foundation (SNSF). W.H. was funded in part by a grant from the SNSF. L.Z. and P.R. were funded in part by a SNSF grant Sinergia (CRSII3_141879).

Appendix A. Supplementary Data

Supplementary data to this article can be found online at http://dx.doi.org/10.1016/j.ebiom.2016.01.019.

References

Amarnath, S., Flomerfelt, F.A., Costanzo, C.M., Foley, J.E., Mariotti, J., Konecki, D.M., Gangopadhyay, A., Eckhaus, M., Wong, S., Levine, B.L., et al., 2010. Rapamycin generates anti-apoptotic human Th1/Tc1 cells via autophagy for induction of xenogeneic GVHD. Autophagy 6, 523–541.

Araki, K., Turner, A.P., Shaffer, V.O., Gangappa, S., Keller, S.A., Bachmann, M.F., Larsen, C.P., Ahmed, R., 2009. mTOR regulates memory CD8 T-cell differentiation. Nature 460, 108–112.

Baan, C.C., van der Mast, B.J., Klepper, M., Mol, W.M., Peeters, A.M.a., Korevaar, S.S., Balk, A.H.M.M., Weimar, W., 2005. Differential effect of calcineurin inhibitors, anti-CD25 antibodies and rapamycin on the induction of FOXP3 in human T cells. Transplantation 80, 110–117.

Berger, C., Jensen, M.C., Lansdorp, P.M., Gough, M., Elliott, C., Riddell, S.R., 2008. Adoptive transfer of effector CD8+ T cells derived from central memory cells establishes persistent T cell memory in primates. J. Clin. Invest. 118, 294–305.

Cao, W., Manicassamy, S., Tang, H., Kasturi, S.P., Pirani, A., Murthy, N., Pulendran, B., 2008. Toll-like receptor-mediated induction of type I interferon in plasmacytoid dendritic cells requires the rapamycin-sensitive PI(3)K-mTOR-p70S6K pathway. Nat. Immunol. 9, 1157–1164.

Cham, C.M., Driessens, G., O'Keefe, J.P., Gajewski, T.F., 2008. Glucose deprivation inhibits multiple key gene expression events and effector functions in CD8+ T cells. Eur. J. Immunol. 38, 2438–2450.

Chi, H., 2012. Regulation and function of mTOR signalling in T cell fate decisions. Nat. Rev. Immunol. 12, 325–338.

Choo, A.Y., Yoon, S.-O., Kim, S.G., Roux, P.P., Blenis, J., 2008. Rapamycin differentially inhibits S6Ks and 4E-BP1 to mediate cell-type-specific repression of mRNA translation. Proc. Natl. Acad. Sci. U. S. A. 105, 17414–17419.

Chresta, C.M., Davies, B.R., Hickson, I., Harding, T., Cosulich, S., Critchlow, S.E., Vincent, J.P., Ellston, R., Jones, D., Sini, P., et al., 2010. AZD8055 is a potent, selective, and orally bioavailable ATP-competitive mammalian target of rapamycin kinase inhibitor with in vitro and in vivo antitumor activity. Cancer Res. 70, 288–298.

Cobbold, S.P., 2013. The mTOR pathway and integrating immune regulation. Immunology 391-398.

Diken, M., Kreiter, S., Vascotto, F., Selmi, A., Attig, S., Diekmann, J., Huber, C., Türeci, Ö., Sahin, U., 2013. mTOR inhibition improves antitumor effects of vaccination with antigen-encoding RNA. Cancer immunol. res. 1, 386–392.

Driessens, G., Zheng, Y., Gajewski, T.F., 2010. Beta-catenin does not regulate memory T cell phenotype. Nat. Med. 16, 513–514 author reply 514-515.

Feldman, M.E., Apsel, B., Uotila, A., Loewith, R., Knight, Z.A., Ruggero, D., Shokat, K.M., 2009. Active-site inhibitors of mTOR target rapamycin-resistant outputs of mTORC1 and mTORC2. PLoS Biol. 7, e38.

Ferrer, I.R., Wagener, M.E., Robertson, J.M., Turner, A.P., Araki, K., Ahmed, R., Kirk, A.D., Larsen, C.P., Ford, M.L., 2010. Cutting edge: rapamycin augments pathogen-specific but not graft-reactive CD8+ T cell responses. J. Immunol. *185*, 2004–2008.

Ferrer, I.R., Araki, K., Ford, M.L., 2011. Paradoxical aspects of rapamycin immunobiology in transplantation. Am. J. Transplant. 11, 654–659.

Fox, C.J., Hammerman, P.S., Thompson, C.B., 2005. Fuel feeds function: energy metabolism and the T-cell response. Nat. Rev. Immunol. 5, 844–852.

Gattinoni, L., Zhong, X.S., Palmer, D.C., Ji, Y., Hinrichs, C.S., Yu, Z., Wrzesinski, C., Boni, A., Cassard, L., Garvin, L.M., et al., 2009. Wnt signaling arrests effector T cell differentiation and generates CD8+ memory stem cells. Nat. Med. 15, 808–813.

Gattinoni, L., Lugli, E., Ji, Y., Pos, Z., Paulos, C.M., Quigley, M.F., Almeida, J.R., Gostick, E., Yu, Z., Carpenito, C., et al., 2011. A human memory T cell subset with stem cell-like properties. Nat. Med. 17, 1290–1297.

Graef, P., Buchholz, V.R., Stemberger, C., Flossdorf, M., Henkel, L., Schiemann, M., Drexler, I., Höfer, T., Riddell, S.R., Busch, D.H., 2014. Serial transfer of single-cell-derived immunocompetence reveals stemness of CD8+ central memory T cells. Immunity 41, 116–126.

Igney, F.H., Krammer, P.H., 2002. Death and anti-death: tumour resistance to apoptosis. Nat. Rev. Cancer 2, 277–288.

Kamphorst, A.O., Ahmed, R., 2013. CD4 T-cell immunotherapy for chronic viral infections and cancer. Immunotherapy 5, 975–987.

Loewith, R., Jacinto, E., Wullschleger, S., Lorberg, A., Crespo, J.L., Bonenfant, D., Oppliger, W., Jenoe, P., Hall, M.N., 2002. Two TOR complexes, only one of which is rapamycin sensitive, have distinct roles in cell growth control. Mol. Cell 10, 457–468.

Lohoff, M., Mak, T.W., 2005. Roles of interferon-regulatory factors in T-helper-cell differentiation. Nat. Rev. Immunol. 5, 125–135.

Lugli, E., Gattinoni, L., Roberto, A., Mavilio, D., Price, D.A., Restifo, N.P., Roederer, M., 2013. Identification, isolation and in vitro expansion of human and nonhuman primate T stem cell memory cells. Nat. Protoc. 8, 33–42.

Markley, J.C., Sadelain, M., 2010. IL-7 and IL-21 are superior to IL-2 and IL-15 in promoting human T cell-mediated rejection of systemic lymphoma in immunodeficient mice. Blood 115, 3508–3519.

Muranski, P., Restifo, N.P., 2009. Adoptive immunotherapy of cancer using $CD4^+$ T cells. Curr. Opin. Immunol. 21, 200–208.

Oberdoerffer, S., Moita, L.F., Neems, D., Freitas, R.P., Hacohen, N., Rao, A., 2008. Regulation of CD45 alternative splicing by heterogeneous ribonucleoprotein, hnRNPLL. Science 321, 686–691.

Pearce, E.L., Walsh, M.C., Cejas, P.J., Harms, G.M., Shen, H., Wang, L.S., Jones, R.G., Choi, Y., 2009. Enhancing CD8 T-cell memory by modulating fatty acid metabolism. Nature 460, 103–107.

Powers, J.M., Trobridge, G.D., 2013. Identification of hematopoietic stem cell engraftment genes in gene therapy studies. J.Stem Cell Res. Ther. 2013, 1–15.

Prlic, M., Bevan, M.J., 2011. Cutting edge: β-catenin is dispensable for T cell effector differentiation, memory formation, and recall responses. J. Immunol. *187*, 1542–1546.

Rao, R.R., Li, Q., Odunsi, K., Shrikant, P.A., 2010. The mTOR kinase determines effector versus memory CD8+ T cell fate by regulating the expression of transcription factors T-bet and eomesodermin. Immunity 32, 67–78.

Slavik, J.M., Lim, D.-g., Burakoff, S.J., Hafler, D.A., 2004. Rapamycin-resistant proliferation of CD8+ T cells correlates with p27kip1 down-regulation and bcl-xL induction, and is prevented by an inhibitor of phosphoinositide 3-kinase activity. J. Biol. Chem. 279, 910–919.

Sukumar, M., Liu, J., Crompton, J., Rao, M., Ji, Y., Finkel, T., Gattinoni, L., Restifo, N., 2013a. Mitochondrial activity regulates T cell memory, self renewal and anti tumor function in CD8+ T cells. J. ImmunoTherapy of Cancer 1, O11-O11.

Sukumar, M., Liu, J., Ji, Y., Subramanian, M., Crompton, J.G., Yu, Z., Roychoudhuri, R., Palmer, D.C., Muranski, P., Karoly, E.D., et al., 2013b. Inhibiting glycolytic metabolism enhances CD8+ T cell memory and antitumor function. J. Clin. Invest. 123, 4479–4488.

Thomson, A.W., Turnquist, H.R., Raimondi, G., 2009. Immunoregulatory functions of mTOR inhibition. Nat. Rev. Immunol. 9, 324–337.

Turner, A.P., Shaffer, V.O., Araki, K., Martens, C., Turner, P.L., Gangappa, S., Ford, M.L., Ahmed, R., Kirk, A.D., Larsen, C.P., 2011. Sirolimus enhances the magnitude and quality of viral-specific CD8+ T-cell responses to vaccinia virus vaccination in rhesus macaques. Am. J. Transplant. 11, 613–618.

van der Windt, G.J.W., Everts, B., Chang, C.-H., Curtis, J.D., Freitas, T.C., Amiel, E., Pearce, E.J., Pearce, E.L., 2012. Mitochondrial respiratory capacity is a critical regulator of CD8+ T cell memory development. Immunity 36, 68–78.

Vermeulen, K., Van Bockstaele, D.R., Berneman, Z.N., 2003. The cell cycle: a review of regulation, deregulation and therapeutic targets in cancer. Cell Prolif. 36, 131–149.

Wherry, E.J., Teichgräber, V., Becker, T.C., Masopust, D., Kaech, S.M., Antia, R., von Andrian, U.H., Ahmed, R., 2003. Lineage relationship and protective immunity of memory CD8 T cell subsets. Nat. Immunol. 4, 225–234.

Xiao, Z., Sun, Z., Smyth, K., Li, L., 2013. Wnt signaling inhibits CTL memory programming. Mol. Immunol. 56, 423–433.

Yang, X., Zhang, M., Ramos, C., Durett, A., Liu, E., Dakhova, O., Liu, H., Creighton, C.J., Gee, A.P., Heslop, H.E., et al. (2014). Closely-related T-memory stem cells correlate with in-vivo expansion of CAR.CD19-T cells in patients and are preserved by IL-7 and IL-15. Blood.

Zhang, Y., Joe, G., Hexner, E., Zhu, J., Emerson, S.G., 2005. Host-reactive CD8+ memory stem cells in graft-versus-host disease. Nat. Med. 11, 1299–1305.

Zheng, Y., Delgoffe, G.M., Meyer, C.F., Chan, W., Powell, J.D., 2009. Anergic T cells are metabolically anergic. J. Immunol. 183, 6095–6101.